Available online at www.sciencedirect.com
ScienceDirect
International Journal of Thermal Sciences 48 (2009) 645–654
International Journal of Thermal Sciences
www.elsevier.com/locate/ijts

Control of a hybrid solar/electric thermal energy storage system

Marc LeBreux *, Marcel Lacroix, Gérard Lachiver

Faculté de génie, Université de Sherbrooke, Sherbrooke (Québec), Canada J1K 2R1

Received 20 February 2008; received in revised form 28 April 2008; accepted 12 May 2008

Available online 12 June 2008

Abstract

A controller for operating a hybrid thermal energy storage system (HTESS) is presented. The storage system accumulates solar energy during sunny days and releases it later at night or during cloudy days and, simultaneously, it stores electric energy during off-peak periods and releases it later during on-peak periods. The control of the system rests on an anticipatory strategy and on a regulation strategy. The anticipatory strategy is based on a fuzzy logic and feedforward controller (FLFFC) that can handle simultaneously the storage and retrieval of both electricity and solar energy. It takes into account the weather forecasts for solar radiation and outside air temperature, and optimizes the off and the on-peak periods for electrical heating. The regulation strategy depends on a PID controller which regulates the air flow from an electric fan in order to maintain the room temperature at the set point. Numerical simulations were conducted over one to three-month winter periods to test the response of the controller. Results indicate that the proposed control system is far superior to traditional control systems. It remains robust and reliable even for cases in which the weather forecasts are of poor reliability and accuracy (5-day horizon weather forecasts with reliability of 50%, −10 K temperature accurate and −50% solar radiation accurate). The performance of the HTESS as well as the thermal comfort of the room is maintained in all situations and at all times. Moreover, the electricity consumption for space heating is minimized and 95% of this electricity is consumed during off-peak hours.

Keywords: Fuzzy logic control; Feedforward control; Weather forecasts; Thermal energy storage; Solar energy; Electric energy

1. Introduction

In northern countries such as Canada, space heating represents the main source of electricity consumption in new homes. As a result, during harsh winter days, the consumption of electricity is increasingly acute in the morning and in the evening and quite often the distribution grid becomes overloaded. One way to alleviate this problem is to shift some of the on-peak demand to off-peak periods by making use of electric storage systems. In these systems, electric energy is conveniently converted into thermal energy and stored in a sensible and/or phase change material during the night and subsequently used the next day. During on-peak periods, the power in the system is automatically shut off and the storage unit discharges its heat to the living space. Of course, to agree to bear the additional cost involved in purchasing and installing a storage system, the customer benefits from lower electricity rates during off-peak periods allowing him to obtain a return on his investment.

On the other hand, an increasing number of home owners, enticed by energy saving measures and concerned with environmental issues, equip their home with solar systems, passive or active. Since the availability of solar energy is usually not coincident with the demand, heat collected from solar radiation must also be stored in a thermal unit. For solar systems however, heat is stored during sunny days and released at night or later during cloudy days.

Recently, a new storage system called a hybrid thermal energy storage system (HTESS) was designed [1]. The storage system can handle simultaneously electric and solar energy. However, when it was tested over long periods of time, conflicting situations arose between both forms of energy yielding, in some cases, overheating of the living space and/or poor thermal performance of the system [1–4].

The objective of the present study is therefore to propose a control system for the HTESS that maximizes its performance. The system handles simultaneously the storage and re-

* Corresponding author.
E-mail address: marc.lebreux@usherbrooke.ca (M. LeBreux).

1290-0729/$ – see front matter
doi:10.1016/j.ijthermalsci.2008.05.006

Nomenclature

A	surface	m^2	
C_p	heat capacity	J/kg K	
C_{14}^r	combinations		
e	wall thickness	m	
E	energy	kWh	
k	thermal conductivity	W/m K	
H	wall and room height	m	
i	iteration value		
I	comfort index	K s	
l	room length	m	
N	reliability parameter (Eq. (11))		
$\dot{m}$	mass flow rate	kg/s	
$\dot{q}$	volumetric heat	W/m^3	
q''	heat flux	W/m^2	
r	allowed periods		
t	time	s	
T	temperature	K	
U	overall heat transfer coefficient	W/m^2 K	
V	volume	m^3	
x	transversal coordinate of HTESS	m	

Greek symbol

ρ	density	kg/m^3

Subscripts

a	air
c	consumption for space heating
co	cooling
el	electrical
fut	forecast
h	previous day
he	heating
in	inlet
max	maximal
0	parietal
out	exterior
ref	set point
sun	solar
w	wall

trieval of both electric and solar energy. It takes into account the accuracy and the reliability of the weather forecasts for solar radiation and outside air temperature, and makes the best with the off and on-peak periods for electricity.

A mathematical model for predicting the thermal behaviour of the HTESS is first presented. The model is next validated with experimental data obtained from a prototype. The control strategy for a fuzzy logic/feedforward controller (FLFFC) is exemplified and the uncertainties of the weather forecasts are introduced. The thermal performance of the HTESS controlled by the FLFFC is then compared to that of a HTESS with no electricity storage and to a traditional electric base board heating system. Finally, the effect of the reliability and accuracy of the weather forecasts on the room temperature, on the electricity consumption and on the cost of space heating is investigated.

2. Modeling the thermal energy storage system

The hybrid thermal energy storage system (HTESS) under investigation is an interior concrete wall facing a bay window (Fig. 1). Heat is stored in the wall via direct solar radiation impinging on the wall surface and via an electric resistance heater embedded in the structure. Air circulation from an electric fan is allowed for adjusting the room temperature.

The mathematical model for the thermal behaviour of the storage system rests on the following assumptions:

- The thermo physical properties of the surrounding air and concrete wall are constant and taken at 300 K;
- The air temperature inside the room is uniform and time dependent;
- Conduction heat transfer in the wall is predominantly one-dimensional (x direction);

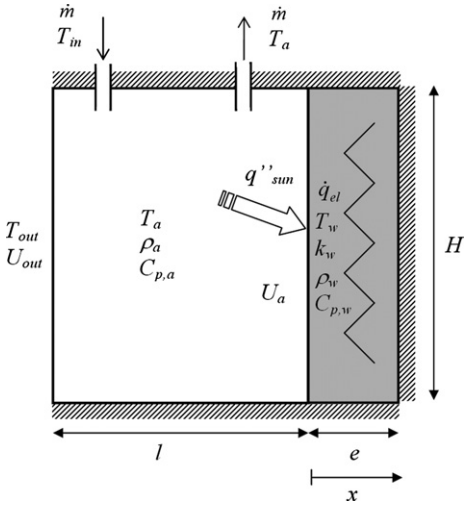

Fig. 1. Schematic of the HTESS.

- The overall heat transfer coefficients U_a and U_{out} remain constant and take into account convection and radiation heat transfer.

Based on the above assumptions, the thermal energy conservation equations and boundary conditions for the room and the wall may be stated as

$$\rho_a V_a C_{p,a} \frac{dT_a}{dt} = \dot{m} C_{p,a}(T_{in} - T_a) + U_a A_a (T_{w,0} - T_a) - U_{out} A_{out} (T_a - T_{out}) \quad (1)$$

$$\rho_w C_{p,w} \frac{\partial T_w}{\partial t} = k_w \frac{\partial^2 T_w}{\partial x^2} + \dot{q}_{el} \quad (2)$$

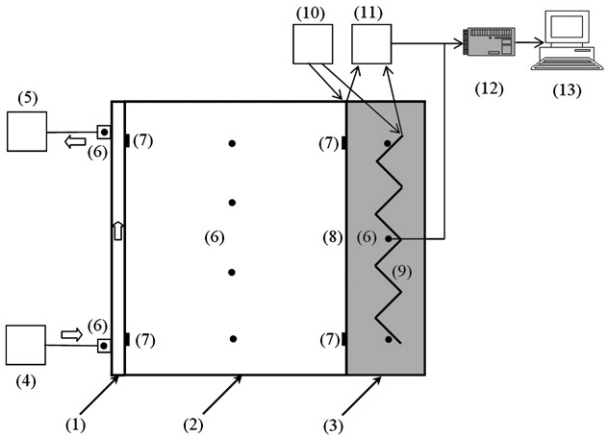

Fig. 2. Schematic of the experimental rig. (1) water jacket, (2) water bath, (3) storage wall, (4) cold water source, (5) tank, (6) thermocouples, (7) heat flux meters, (8) ribbon heaters, (9) electric wire, (10) power supply, (11) power transducers, (12) data acquisition unit, (13) computer.

$$-k_{\mathrm{w}}\left.\frac{\partial T_{\mathrm{w}}}{\partial x}\right|_{x=0} = q''_{\mathrm{sun}} - U_{\mathrm{a}}(T_{\mathrm{w},0} - T_{\mathrm{a}}) \tag{3}$$

$$\left.\frac{\partial T_{\mathrm{w}}}{\partial x}\right|_{x=e} = 0 \tag{4}$$

$T_{\mathrm{a}}(t)$ is the temperature of the room and $T_{\mathrm{w}}(x,t)$ is the temperature of the wall.

The above system of equations is solved straightforwardly with a 4th order Runge–Kutta scheme.

3. Validation

The above numerical model was first tested and compared to analytical solutions. A series of simulations was also conducted to ensure that the solutions are grid and time step independent.

Next, an experimental rig was set up to further check the validity of the numerical model. The experimental prototype of the storage system shown in Fig. 2, scale 1:6, consists of a water bath 0.5 m high, 0.5 m deep and 0.15 m wide with an adjoining 0.035 m thick storage wall made of concrete. The water reservoir is used to simulate the thermal behaviour of the room. Moreover, an aluminium jacket, cooled with water, is used to represent the heat loss from the window. Thermal energy is stored in the wall by means of ribbon copper heaters covering uniformly its external surface. These surface heaters mimic the effect of direct solar radiation. An electric wire embedded in the wall structure also simulates heat storage from electric sources. The electric power dissipated in the heaters is measured by power transducers and are controlled by a power supply. Temperatures are measured with an accuracy of ± 0.5 K by means of 32 copper-constantan thermocouples (type T) located in the water bath, in the water jacket, and distributed in the storage wall. Four heat flux meters were also used to estimate the surface heat fluxes. The instrumentation is connected to a data acquisition system and the data is processed with the software LABVIEW from National Instruments.

Several laboratory experiments were carried out for different heating and cooling scenarios and numerical simulations were conducted simultaneously to mimic the observed thermal behaviour of the storage system. As an example, Fig. 3 compares the temporal variation of the predicted and measured temperatures of the water bath for a scenario in which both ribbon and embedded heaters were employed. In this experiment, 250 watts are first supplied to the ribbon heaters for a time period of 4788 seconds followed by a cooling period of 4788 seconds. Then, the 550 W electric heater embedded in the concrete wall is turned on for a time period of 4788 seconds and finally turned off. The results shown in Fig. 3 reveal that the agreement between the numerical predictions and the data is well within the experimental uncertainties. These experimental uncertainties result from the temperature measurement errors made on the experimental rig. They are not concerned with the weather forecasts uncertainties discussed in Section 5.

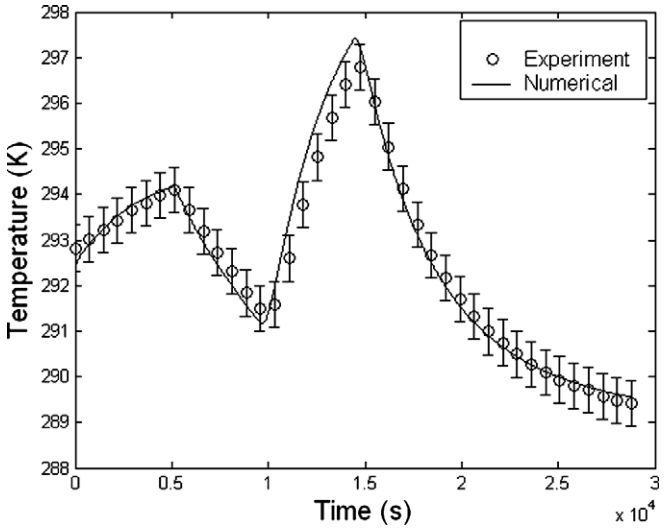

Fig. 3. Predicted and measured temperatures of the water bath.

4. Control strategy

Recent studies have shown that traditional PID controllers are, in many cases, inadequate for the control of solar and electric storage systems [5–15]. Such controllers cannot anticipate the disturbance inputs nor the time evolution of the storage system and, as a result, they often lead to the overheating of the room. Moreover, to achieve similar performances, PID parameters must be tuned for every new room.

Fuzzy logic controllers (FLC) overcome some of these drawbacks. They rely on simple linguistic rules that allow them to handle easily meteorological forecasts. Consequently, heat storage may be carried out in such a way as to avoid the problems associated with the overheating of the storage medium and of the adjacent room. Fuzzy inference systems are very effective for modeling nonlinear systems especially when uncertainty knowledge is involved.

Feedforward controllers (FFC) are, on the other hand, particularly suitable for controlling storage systems with large thermal inertia (long time constant). In spite of the fact that their behaviour rests on standard mathematical models, they can still be operated while taking into account weather forecasts.

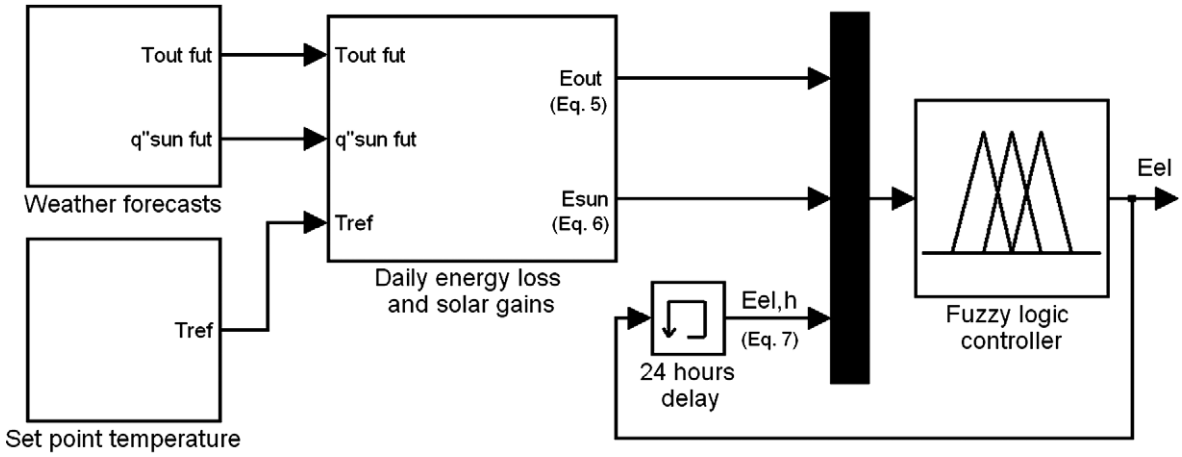

Fig. 4. Fuzzy logic controller.

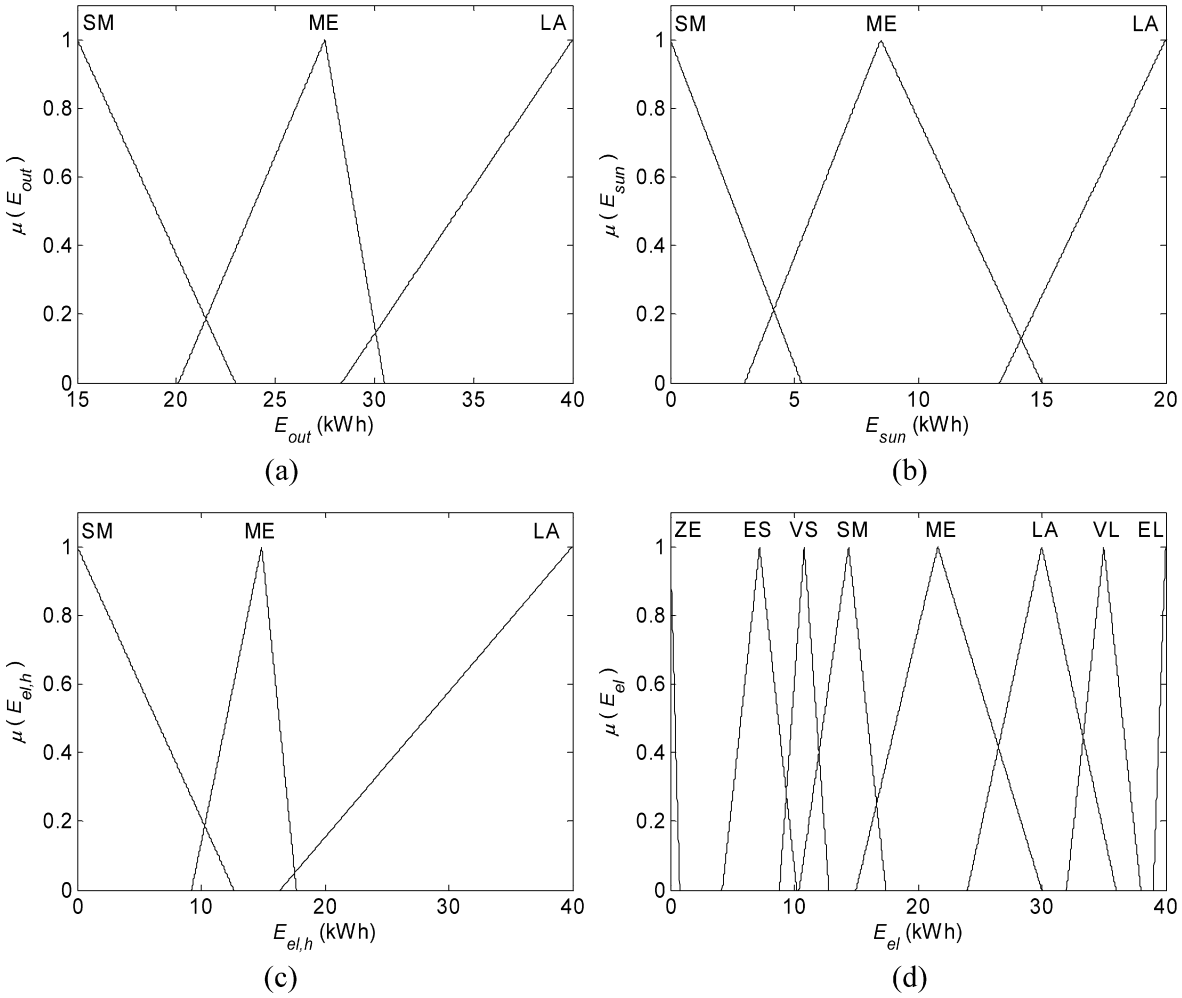

Fig. 5. Triangular-shaped membership functions. SM: small; ME: medium; LA: large; ZE: zero; ES: extremely small; VS: very small; VL: very large; EL: extremely large.

Based on the above observations, a system that relies on a fuzzy logic and a feedforward controller is proposed to handle simultaneously the storage and retrieval of both electricity and solar energy in the HTESS (anticipatory strategy). The FLC is employed for estimating the amount of thermal electric energy (in kWh) to be stored for the next 24 hours. With this information, the FFC is then used to determine the electric power consumption profile (in kW) of the heating element for the off-peak hour periods. Moreover, in order to maintain the temperature of the room at the set point, an electric fan and a PID controller are used (regulation strategy).

As shown in Fig. 4, the amount of thermal electric energy to be stored in the HTESS for the current day is E_{el}. The inputs to the FLC controller are the estimated energy loss from the HTESS during that day E_{out}, the forecasted solar radiation E_{sun} and the amount of thermal electric energy stored during the previous day $E_{el,h}$. These input parameters are calculated with the following relations:

$$E_{out} = \int_{t}^{t+24h} \left[U_{out} A_{out} (T_{ref} - T_{out,fut})\right] dt \quad (5)$$

$$E_{sun} = \int_{t}^{t+24h} (q''_{sun,fut} A_a)\, dt \quad (6)$$

$$E_{el,h} = \int_{t-24h}^{t} (\dot{q}_{el} V_w)\, dt \quad (7)$$

The inputs and output of the FLC are fuzzified using 3 and 8 triangular membership functions respectively (Fig. 5). These simple functions were retained since they can be easily tuned ad hoc to minimize the temperature difference between the predictions and the set point for the room temperature, even when the controller does not rely on a regulation strategy. They also yield the best results for minimizing the energy consumption. The fuzzy controller structure is a Mamdani type FLC using a MIN-MAX inference technique. The adopted defuzzification method, for fuzzy output E_{el}, is based on the determination of the centroïd method [16]. The fuzzy controller model comprises 27 linguistic rules that were derived from our own expertise. These rules are provided in Table 1. More sophisticated fuzzy structures and design techniques were not necessary since the proposed FLC was easily implemented and tuned while providing stable results.

From the amount of thermal electric energy to be stored in the HTESS, a FFC next determines the daily electric power consumption profile for the heating element $\dot{q}_{el}$ that minimizes the comfort index I. This index is defined as

$$I = \int_{t}^{t+24h} |T_{ref} - T_{a,fut}|\, dt \quad (8)$$

The overall FFC strategy is summarized in Fig. 6. It is assumed that the heating element can be turned on only during the 7 off-

Table 1
Linguistic rules of the FLC

Rule	If E_{out} is	And E_{sun} is	And $E_{el,h}$ is	Then E_{el} is
1	SM	SM	SM	SM
2	SM	SM	ME	SM
3	SM	SM	LA	ES
4	SM	ME	SM	SM
5	SM	ME	ME	SM
6	SM	ME	LA	ES
7	SM	LA	SM	ES
8	SM	LA	ME	ZE
9	SM	LA	LA	ZE
10	ME	SM	SM	ME
11	ME	SM	ME	ME
12	ME	SM	LA	ES
13	ME	ME	SM	ME
14	ME	ME	ME	SM
15	ME	ME	LA	ES
16	ME	LA	SM	ES
17	ME	LA	ME	ZE
18	ME	LA	LA	ZE
19	LA	SM	SM	LA
20	LA	SM	ME	LA
21	LA	SM	LA	VL
22	LA	ME	SM	EL
23	LA	ME	ME	EL
24	LA	ME	LA	ME
25	LA	LA	SM	VS
26	LA	LA	ME	VS
27	LA	LA	LA	ES

SM: small; ME: medium; LA: large; ZE: zero; ES: extremely small; VS: very small; VL: very large; EL: extremely large.

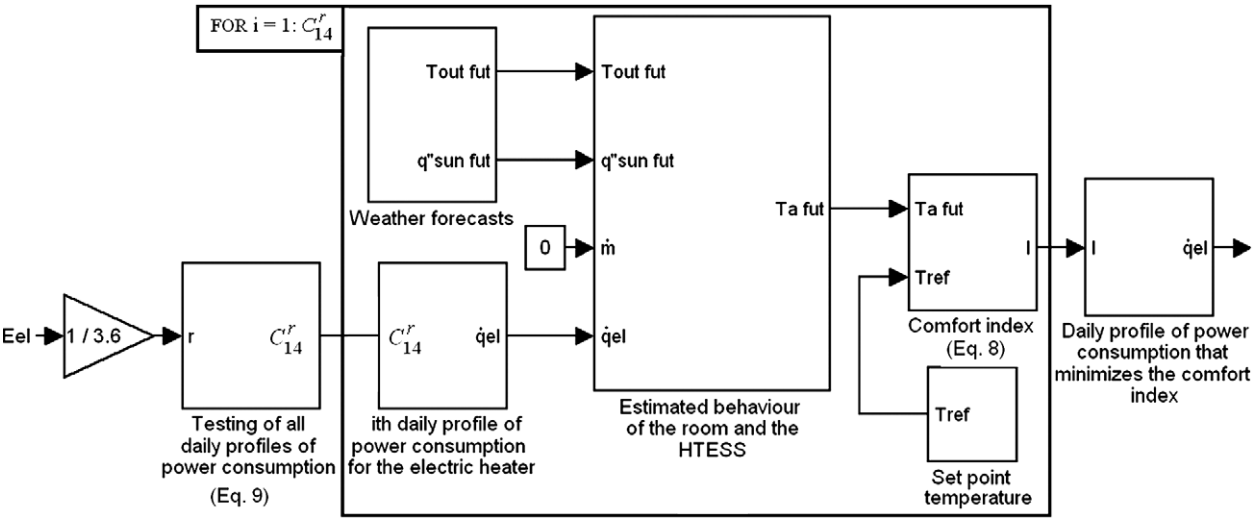

Fig. 6. Feedforward controller.

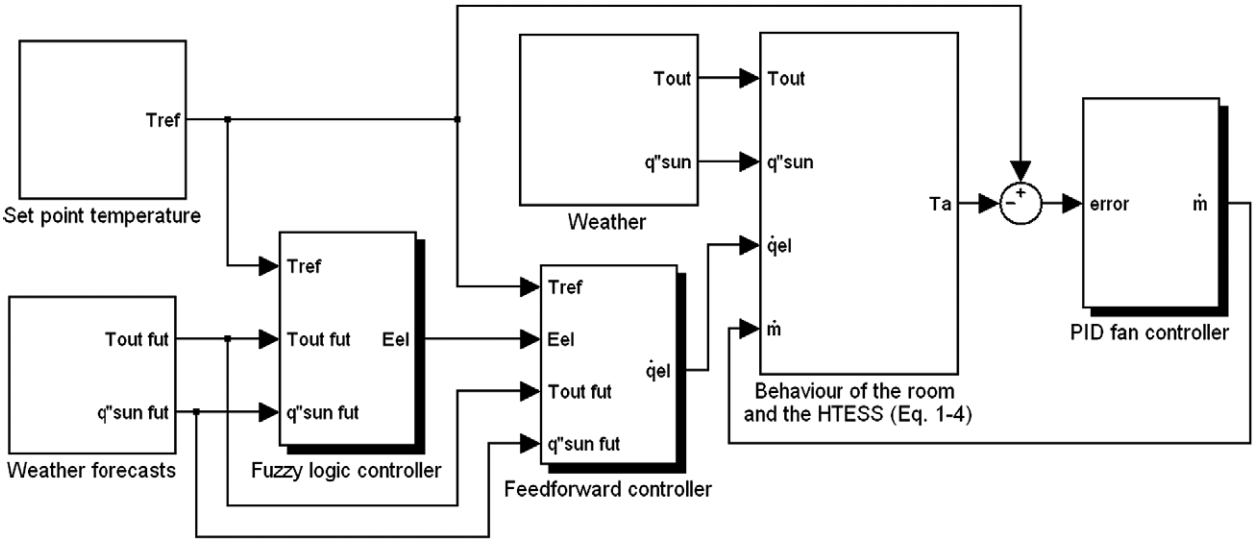

Fig. 7. Overall control strategy for the HTESS.

peak hours, that is from 02h00 to 06h00 and from 13h00 to 16h00. These time periods are divided into fourteen 30-minute daily time periods. By dividing the output of the FLC (in kWh) by 3.6 kWh, the value r corresponds to the number of periods, over 14, when electric storage is allowed. As a result, the number of different combinations for the daily consumption profiles is given by

$$C_{14}^{r} = \frac{14!}{r!(14-r)!} \tag{9}$$

Each of these combinations is tested with the weather forecasts and checked with the mathematical model for the room and the HTESS. The estimated room temperature $T_{\mathrm{a,fut}}$ is then employed for the calculation of the comfort index I (Eq. (8)). The daily profile that minimizes this index is retained.

The input of the PID controller is the temperature error, defined as the difference between the set point temperature and the room temperature. As for the output of the PID, it is the mass flow rate of air supplied by the electric fan and it is determined from

$$\dot{m} = K_p(T_{\mathrm{ref}} - T_{\mathrm{a}}) + K_i\left[\int (T_{\mathrm{ref}} - T_{\mathrm{a}})\,dt\right] + K_d\left[\frac{d(T_{\mathrm{ref}} - T_{\mathrm{a}})}{dt}\right] \tag{10}$$

The inlet air may be heated or cooled according to the average room temperature.

The overall controller strategy for the HTESS is depicted in Fig. 7.

The above controller was developed using "exact" weather forecasts, i.e. equal to measured meteorological data. In the next section, we examine the effect of the uncertainties in the weather forecasts on the performance of the HTESS control system, without making any changes to its structure.

5. Uncertainties of the weather forecasts

The uncertainties in the weather forecasts are expressed in terms of the reliability and the accuracy of the data. From the weather data provided by Environment Canada [17], the reliability is defined here as the daily percentage of the forecasted weather data that correspond to the measured data, that is,

$$\text{reliability} = \frac{\sum_{i=1}^{24} N(i)}{24} \times 100 \tag{11}$$

where $N(i) = 1$ when the forecasted datum corresponds to the measured datum and $N(i) = 0$ otherwise. When $N(i) = 0$, the difference between the forecasted and the measured datum is defined as the accuracy. The accuracies for the temperature and the solar radiation are expressed respectively as

$$T_{\mathrm{out,fut}}\ \text{accuracy} = T_{\mathrm{out,fut}}(\text{forecasted}) - T_{\mathrm{out,fut}}(\text{measured}) \tag{12}$$

$$q''_{\mathrm{sun,fut}}\ \text{accuracy} = \frac{q''_{\mathrm{sun,fut}}(\text{forecasted}) - q''_{\mathrm{sun,fut}}(\text{measured})}{q''_{\mathrm{sun,fut}}(\text{measured})} \times 100 \tag{13}$$

Every day, the number of forecasted data different from the measured data, i.e. $24 - \sum_{i=1}^{24} N(i)$, are distributed randomly over a 24-hour time period.

At Environment Canada, the reliability of the weather forecasts for a five day horizon lies between 80% and 85% for the first two days and then drop to 70% for the third day, to 60% for the fourth day, and to 50% for the fifth day. On the other hand, the accuracy on the temperatures is ± 2 K for the first day and increases to ± 5 K for the fifth day [18]. Since no information is provided by Environment Canada on the accuracy of the forecasted solar heat fluxes, an accuracy ranging from $\pm 10\%$ to $\pm 50\%$ for time horizon of one to five days was assumed in the present study.

6. Results and discussion

Numerical simulations were conducted to assess the performance of the proposed control system. The main parameters characterizing the room and the HTESS are provided in Table 2.

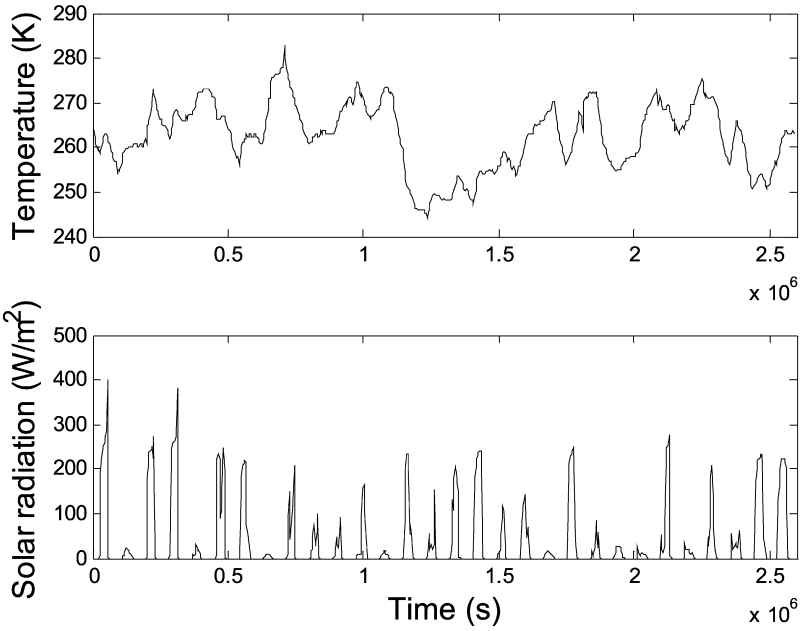

Fig. 8. Exact weather forecasts for the month of January (Montréal, Canada).

Table 2
Parameters for the simulations

Parameter	Magnitude
e	0.3 m
H	3 m
l	5 m
A_a	9 m^2
A_{out}	9 m^2
U_a	8 W/m^2 K
U_{out}	4 W/m^2 K
$T_{in,he}$	308 K
$T_{in,co}$	288 K
$(\dot{q}_{el} V_w)_{max}$	7200 W
$\dot{m}_{max}$	0.14 kg/s

The thermo physical properties of the concrete wall and of the air were taken from Ref. [19].

Simulations were first carried out using the meteorological data for a time period extending to three consecutive winter months, i.e. from January 1st to March 31st for the city of Montréal, Canada [17]. The main results are summarized in Table 3 in terms of the total electricity consumption for space heating. Three heating systems are compared: (1) a traditional base board electric heating system with no thermal storage, (2) a thermal energy storage system with no electric storage, i.e. only solar energy is stored in the HTESS and, (3) the proposed system, i.e. a HTESS with a FLFFC. It is assumed here that the electricity consumption for the base board electric system corresponds to the heat losses from the room. Therefore, it may be calculated according to

$$E_c = \int_t^{t+24h} \left[U_{out} A_{out} (T_{ref} - T_{out})\right] dt \tag{14}$$

Table 3
Electricity consumption for space heating: three consecutive winter months with exact weather forecasts

Case	E_c (off-peak hours) (kWh)	E_c (on-peak hours) (kWh)	E_c (total) (kWh)
Base board system	1323	719	2042
HTESS, no electric storage	806	555	1361
HTESS/FLFFC	1469	94	1563

For the HTESS, the electricity consumption is evaluated with

$$E_c = \int_t^{t+24h} \left[\dot{q}_{el} V_w + \dot{m}_{he} C_{p,a} (T_{in} - T_a)\right] dt \tag{15}$$

Examination of Table 3 reveals that the HTESS reduces substantially the electricity consumption compared to that of a traditional base board system. The HTESS with no electric storage appears to be the most efficient system in terms of the total electricity consumption. 41% of the electricity is consumed however during peaks hours. When the HTESS is operated with a FLFFC, the total electricity consumption rises by 13%, but 94% of the electricity is consumed during off-peak hours which is a definite advantage.

Next, a series of simulations for the month of January was conducted to examine the effect of the uncertainties in the weather forecasts on the response of the FLFFC and on the thermal behaviour of the HTESS. The time varying average temperatures and solar radiation (direct and diffuse [20]) for these data hereinafter referred as the "exact" weather forecasts (reliability of 100% and accuracy of 0 K on temperature and 0% on solar radiation) are depicted in Fig. 8. A wide range of reliabilities and accuracies in the weather forecasts were investigated. Reliabilities ranged from 85% down to 50%, and accuracies in

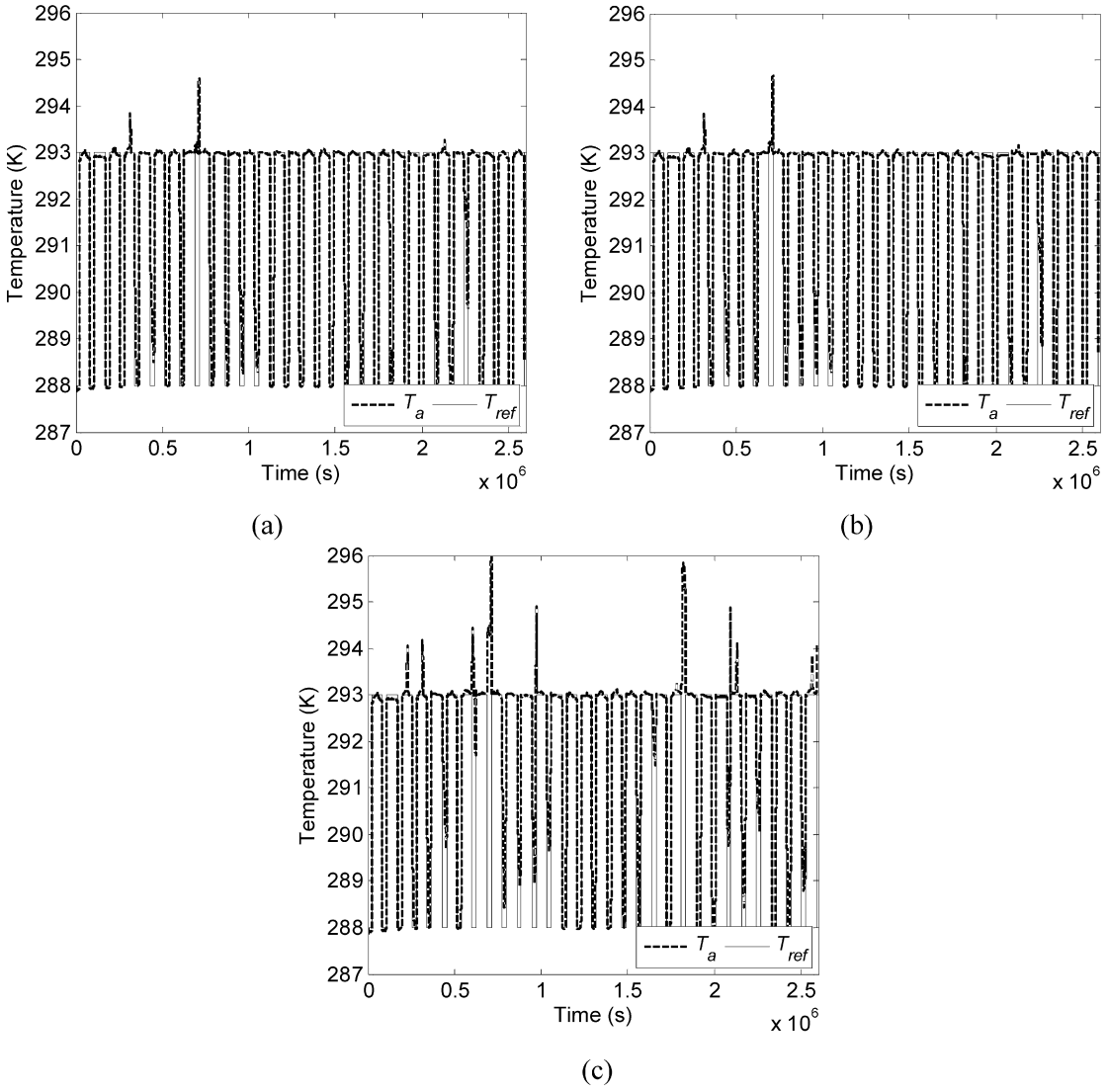

Fig. 9. Set point temperature and predicted room temperature controlled by the overall strategy. (a) no uncertainties. (b) 85% reliable, 2 K temperature accurate and 20% solar radiation accurate. (c) 50% reliable, −10 K temperature accurate and −50% solar radiation accurate.

temperatures and solar radiations ranged from ±2 K to ±10 K and from ±10% to ±50% respectively.

Due to the random distribution in the generation of the uncertainties, each simulation was run five times for a given combination of reliability and accuracy. As a result, extensive computational resources were needed and more than 2400 simulations were carried out on a super computer comprising 872 Intel P4 3.2 GHz central processing units [21]. Each simulation required 2 hours of computational time per CPU.

As an example, Fig. 9 shows the predicted time varying room temperature for three different test cases when the overall control strategy is used. In the first test case (Fig. 9(a)), the "exact" weather forecasts are used. In the second test case (Fig. 9(b)), the weather forecasts are 85% reliable, 2 K temperature accurate and 20% solar radiation accurate. In the third test case (Fig. 9(c)), the weather forecasts are 50% reliable, −10 K temperature accurate and −50% solar radiation accurate. Two observations can be made from these figures. First, for the three test cases, the room temperature is maintained at the set point at all time, except for few nights when the room must be cooled (the electric fan was shut off in this case). Second, the controller response for the room temperature is clearly unaffected by the uncertainties in the weather forecasts.

Fig. 10 illustrates the corresponding variation of the total electricity consumption of the HTESS for space heating as a function of the temperature and of the solar radiation accuracy. The electricity consumption is estimated with Eq. (15). This figure reveals that the electricity consumption is also nearly insensitive to the uncertainties in the weather forecasts. For typical 24-hour horizon weather forecasts, the uncertainties have an insignificant effect on the electricity consumption (Table 4). In fact, for the worst case scenario simulated, i.e., for 5-day horizon weather forecasts with reliability of 50%, −10 K temperature accurate and −50% solar radiation accurate, the total electricity consumption showed a maximum difference of 13% with that of the reference test case (reliability of 100%). Indeed, E_{out} (Eq. (5)) and E_{sun} (Eq. (6)) behave as low-pass

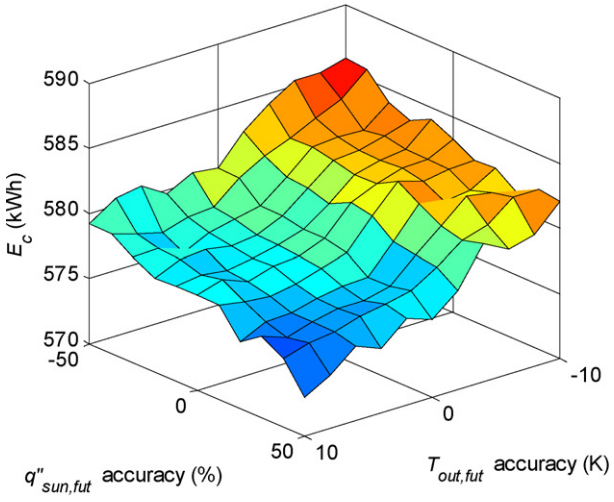

Fig. 10. Total energy consumption versus temperature and solar radiation accuracies for a reliability of 85%.

Table 4
Effect of the weather forecast uncertainties on electricity consumption for space heating for the month of January (Montréal, Canada)

Reliability (%)	$T_{out,fut}$ accuracy (K)	$q''_{sun,fut}$ accuracy (%)	E_c (off-peak hours) (kWh)	E_c (on-peak hours) (kWh)	E_c (total) (kWh)
100	0	0	523	56	579
85	2	0	520	58	578
	0	20	518	59	577
	2	20	517	60	577
	−2	0	527	54	581
	0	−20	524	55	579
	−2	−20	527	54	581

Table 5
Electricity consumption for different space heating systems (with uncertainties in weather forecasts)

Heating system	E_c (off-peak hours) (kWh)	E_c (on-peak hours) (kWh)	E_c (total) (kWh)
Base board system	489	264	753
HTESS, no electric storage	321	217	538
HTESS/FLFFC (worst case scenario*)	635	29	664

* Reliability = 50%, $T_{out,fut}$ accuracy = −10 K and $q''_{sun,fut}$ accuracy = −50%.

filters thus allowing the FLFFC to achieve the present performance.

Table 5 compares the electricity consumption of a traditional base board electric heating system with no storage, of the HTESS with no electric storage (solar energy only), and of the HTESS/FLFFC operated in the worst case scenario. The electricity consumption for the base board electric system is calculated from Eq. (14). The electricity consumption for the HTESS with no electric storage is given by Eq. (15). It is seen from this table that even when the most unreliable and inaccurate weather forecasts are employed, the performance of the HTESS/FLFFC system remains unmatched. Its electricity consumption is smaller than that of the base board system and, furthermore, 95% of the electricity is consumed during off-peak hours, compared to 60% for the HTESS with no electric storage. When these energy consumptions are translated into monetary units using a conservative time-of-use rate scheme for which the on-peak hour rates are twice that of off-peak hours, the HTESS/FLFFC system is unquestionably more attractive than the base board system and the HTESS with no electric storage (Table 6).

Table 6
Electricity costs with time-of-use rates (with uncertainties in weather forecasts)

Heating system	Cost (off-peak hours) (Monetary unit)	Cost (on-peak hours) (Monetary unit)	Cost (total) (Monetary unit)
Base board system	489 × 1	264 × 2	1017
HTESS, no electric storage	321 × 1	217 × 2	755
HTESS/FLFFC (worst case scenario)	635 × 1	29 × 2	693

7. Concluding remarks

A controller for operating a hybrid thermal energy storage system (HTESS) was presented. The storage system accumulates solar energy during sunny days and releases it later at night or during cloudy days and, simultaneously, it stores electric energy during off-peak periods and releases it later during on-peak periods. The control of the system rests on an anticipatory strategy and on a regulation strategy. The anticipatory strategy is based on a fuzzy logic and feedforward controller (FLFFC) that can handle simultaneously the storage and retrieval of both electricity and solar energy. It takes into account the weather forecasts for solar radiation and outside air temperature, and optimizes the off and the on-peak periods for electrical heating. The regulation strategy depends on a PID controller which regulates the air flow from an electric fan in order to maintain the room temperature at the set point. Numerical simulations were conducted over one to three-month winter periods to test the response of the controller. Results indicate that the proposed control system is far superior to traditional control systems. It remains robust and reliable even for cases in which the weather forecasts are of poor reliability and accuracy (5-day horizon weather forecasts with reliability of 50%, −10 K temperature accurate and −50% solar radiation accurate). The performance of the HTESS as well as the thermal comfort of the room is maintained in all situations and at all times. Moreover, the electricity consumption for space heating is minimized and 95% of this electricity is consumed during off-peak hours.

Acknowledgements

The authors gratefully acknowledge the financial support of the Ministère des Ressources naturelles du Québec (project PADTE) and of the Natural Sciences and Engineering Research Council of Canada. They also thank Michel Barrette and Minh-Nghia Nguyen for their help in using the super computer facilities.

References

[1] Z. Ait Hammou, M. Lacroix, A hybrid thermal energy storage system for managing simultaneously solar and electric energy, Energy Conversion and Management 47 (3) (2006) 273–288.

[2] R.C. Winn, C.B. Winn, Optimal control of auxiliary heating of passive-solar heated buildings, Solar Energy 35 (5) (1985) 419–427.

[3] A.A. Argiriou, I. Bellas-Velidis, C.A. Balaras, Development of a neural network heating controller for solar buildings, Neural Networks 13 (7) (2000) 811–820.

[4] G. Bakos, Energy management method for auxiliary energy saving in a passive-solar-heated residence using low-cost off-peak electricity, Energy and Buildings 31 (3) (2000) 237–241.

[5] A.K. Athienitis, T.Y. Chen, Comparison of control strategies for floor heating, Part 2, ASHRAE Transactions 108 (2002) 1005–1013.

[6] T. Takakura, T.O. Manning, G.A. Giacomelli, W.J. Roberts, Feedforward control for a floor heat greenhouse, Transactions of the ASAE 37 (3) (1994) 939–945.

[7] D. Kolokotsa, D. Tsiavos, G.S. Stavrakakis, K. Kalaitzakis, E. Antonidakis, Advanced fuzzy logic controllers design and evaluation for buildings' occupants thermal-visual comfort and indoor air quality satisfaction, Energy and Buildings 33 (6) (2001) 531–543.

[8] D. Kolokotsa, K. Niachou, V. Geros, K. Kalaitzakis, G.S. Stavrakakis, M. Santamouris, Implementation of an integrated indoor environment and energy management system, Energy and Buildings 37 (1) (2005) 93–99.

[9] A.V. Sebald, D. Munoz, On eliminating peak load auxiliary energy consumption in passive solar residences during winter, Solar Energy 39 (4) (1987) 307–319.

[10] D. Kolokotsa, Comparison of the performance of fuzzy controllers for the management of the indoor environment, Building and Environment 38 (12) (2003) 1439–1450.

[11] R.E. Rink, Optimal operation of solar heat storage with off-peak energy price incentive, Optimal Control Applications & Methods 15 (1994) 251–266.

[12] G.C. Bakos, Improved energy management method for auxiliary electrical energy saving in a passive-solar heated residence, Energy and Buildings 34 (7) (2002) 699–703.

[13] T.Y. Chen, Application of adaptive predictive control to a floor heating system with a large thermal lag, Energy and Buildings 34 (1) (2002) 45–51.

[14] X. Lü, M. Viljanen, Controlling building indoor temperature and reducing heating cost through night heating electric stove, Energy and Buildings 33 (8) (2001) 865–873.

[15] B. Thomas, M. Soleimani-Mohseni, P. Fahlén, Feedforward in temperature control of buildings, Energy and Buildings 37 (7) (2005) 755–761.

[16] T.J. Ross, Fuzzy Logic with Engineering Applications, second edition, John Wiley & Sons, New York, 2004, 650 pp.

[17] http://meteo.ec.gc.ca.

[18] http://www.smc-msc.ec.gc.ca/cmc/verification/verification/index_f.html.

[19] F.P. Incropera, D.P. Dewitt, Fundamentals of Heat and Mass Transfer, fifth edition, John Wiley & Sons, New York, 2002, 981 pp.

[20] J.A. Duffie, W.A. Beckman, Solar Engineering of Thermal Processes, John Wiley & Sons, New York, 1980, 762 pp.

[21] http://www.ccs.usherbrooke.ca.